Vol. 82 No. 6 pp. 1141–1145 ACTA GEOLOGICA SINICA Dec. 2008

An AFM Observation on Fossil Cytoplasm

WANG Xin[1, *], YU Junping[2] and FANG Xiaohong[2]

1 *State Key Laboratory of Palaeobiology and Stratigraphy, Nanjing Institute of Geology and Palaeontology, Nanjing 210008, China*

2 *Key Laboratory of Molecular Nanostructure and Nanotechnology, Institute of Chemistry, Beijing 100080, China*

Abstract: Fossil cytoplasm is a new research topic of interest in paleobotany. Atomic force microscope (AFM) is a new technology applied widely in physics and biology; however, it is rarely used in paleontology. Here we applied AFM for the first time to study fossil cytoplasm. The results indicate that the fossil cytoplasm is heterogeneous and full of ultrastructures, just like extant cytoplasm, and that the application of AFM, especially in combination with other techniques, can reveal the subcellular details of fossil plants with more confidence.

Key words: cytoplasm, fossil, AFM, plant

1 Introduction

Traditionally, paleobotany is a science that studies physiologically inactive parts of fossil plants, such as cell wall and cuticle, leaving an increasing gap between itself and other plant sciences. Fortunately, the good preservation of fossil plants began to attract more attention of scientists since the first report of cytoplasm relics by Darrah (Darrah, 1938). Subsequently, large number of discoveries have been made (Mamay, 1957; Eisenack, 1965; Gould, 1971; Satterthwait and Schopf, 1972; Millay and Eggert, 1974; Taylor and Millay, 1977; Niklas et al., 1978; Schönhut et al., 2004; Wang, 2004, 2006, 2007; Collinson et al., 2005; Koller et al., 2005; Ozerov et al., 2006; Wang and Cui, 2007; Wang et al., 2007). Many aspects of fossil plants previously inaccessible to paleobotanists, such as physiological activity, become practical research topics for paleobotany now (Wang et al., 2007).

Atomic force microscope (AFM) has become a popular tool since the 1990s. On one hand, it has been extensively applied in biology (Han et al., 1997; Hizume et al., 2002; Yoshimura et al., 2003; Jalili and Laxminarayana, 2004; Chen et al., 2005; Tiribilli et al., 2005; Muys et al., 2006, among others). These applications of AFM, especially when coupled with conventional light microscope, reveal many aspects of biological processes, and sometimes in real-time. On the other hand, Kempe et al. (Kempe et al., 2002) have applied AFM in the study on the Precambrian microscopic fossils. However, AFM technology has never been applied to fossil plants yet, much less to fossil plant cytoplasm.

Here we used AFM to observe cells in a fossil plant that is more than 15 million years old (Ma). The observation not only demonstrates the good preservation of the fossil cytoplasm but also reveals more ultrastructures within cells. The cytoplasm is heterogeneous with granules and membrane-bound subcellular structures, just as expected for the cells in living plants. The outcome of this AFM observation implies further potential application of AFM in paleontology.

2 Material and Method

The fossil material was a charcoalified coniferous cone collected from the Clarkia fossil locality (Fig. 1, P33, 47° 01′N, 116°25′W, Wang et al., 2007), Idaho, USA in May, 2005. The fossil was embedded in a stratum of gray siltstone of diatom with a Miocene age (15–17 Ma, Wang et al., 2007). The specimen was separated from the sediment matrix by cleaning in 20% HCl, 40% HF, and then 20% HCl again. This process was repeated twice to ensure the complete removal of minerals. The cone was photographed using a Leica MZ-16A stereomicroscope with a digital camera (Plate I, Fig. a). A tiny piece of the cone scale was removed from the cone and embedded in an Epon 812 for thin and ultrathin sections. Two-micron-thick sections were cut with a Reichert-Jung Ultracut E ultramicrotome using a glass knife for light microscopy (Fig. 2). For AFM observation, the ultrathin/thin sections were processed with saturated solution of NaOH in

* Corresponding author. E-mail: brandonhuijunwang@gmail.com

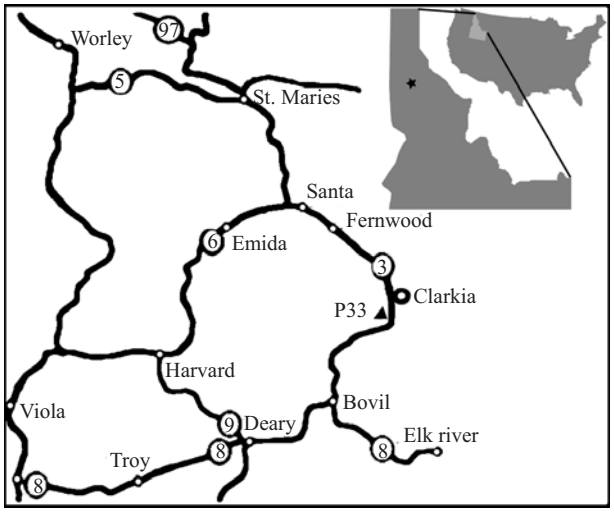

Fig. 1. Map of the fossil locality (P33) at Clarkia in Idaho, USA. The black triangle indicates where the fossil was collected (47°01′N, 116°25′W).

ethanol alcohol to remove the embedding resin (Tiribilli et al., 2005). These sections were then observed in air using a PicoSPM II (Molecular Imaging, Tempe, AZ, USA) with a PicoScan 3000 controller in tapping mode using silicon tips (Plate I, Figs. e-h) and Nanoscope IV (Digital Instruments, Santa Barbara, CA) in contact mode (Fig. 2; Plate I, Figs. i-k). The PicoSPM had an inverted light microscope integrated, so both light microscope and AFM observations could be performed simultaneously on the sample. The topography and amplitude/phase images were all gleaned in the same area at the same time. Afterwards the same material was observed and photographed using an Olympus polarizing microscope (model BX51-75J21PO standard set) (Plate I, Fig. b). Then, using the images taken using light microscopes and AFM as a guidance, the same spots on the palladium coated sections were located and observed using a Leo1530 VP SEM for comparison (Plate I, Figs. c-d). The outcomes of light microscope, AFM and SEM observations were saved in TIFF format. These pictures were pieced together for publication in Photoshop 7.0.

The specimen was numbered as PB20715, and deposited in the paleobotanical collection of Nanjing Institute of Geology and Palaeontology, Nanjing, China.

3 Results

The fossil material is a small premature cone, about 5.5 mm long and 3.5 mm in diameter (Plate I, Fig. a). Cone scales are attached to the cone axis almost at a right angle and converge to the apex of the cone (Plate I, Fig. a). Two-micron-thick thin sections are made of the cone scale. The cells in the cone scale have their cytoplasm preserved (Plate I, Figs. b-d). A series of AFM images at various magnifications show that there are subcellular structures preserved (Plate I, Figs. f-k). The information of topography and amplitude has been collected from the same area simultaneously (Plate I, Fig. e-h). The information of topography and phase was also collected simultaneously (Plate I, Figs. i-k). AFM topographical images (left panels in Plate I, Figs. f-k) record height variations, which are evident in the cross sections (Plate I, Fig. e). The corresponding amplitude images (right panels in Plate I, Figs. e-h) show the variations in height gradient. The phase images show the variations of physical/chemical properties of the fossil cytoplasm (right panels in Plate I, Figs. i-k). The cytoplasm appears to be composed of granules of various sizes (Plate I, Fig. h). The granules in the nucleus-like region are about 110–330 nm in diameter, while those in the cytoplasm matrix are much smaller (16–30 nm) (Plate I, Fig. h). Some of the organelle has two membranes around, which appear as two parallel curves (Plate I, Fig. i). Membrane patches are frequently seen distributed in the cytoplasm (Plate I, Figs. j-k), and their outlines are more conspicuous in the phase images (right panels in Plate I, Figs. j-k).

4 Discussion

In left panels of Plate I, Figs. f-k, the images demonstrate the microtopographical variations of the sample. These images demonstrate similarity to those of the cut cells of extant materials (Chen et al., 2005, fig. 4). As seen in the freezing-etching images of the extant cells (Moor and Mühlethaler, 1963; Fineran, 1978; Canny and Huang, 2006; Fernando et al., 2006), the cell surface cut by sectioning knife is not even but demonstrates a certain pattern in the elevation variations that are related with

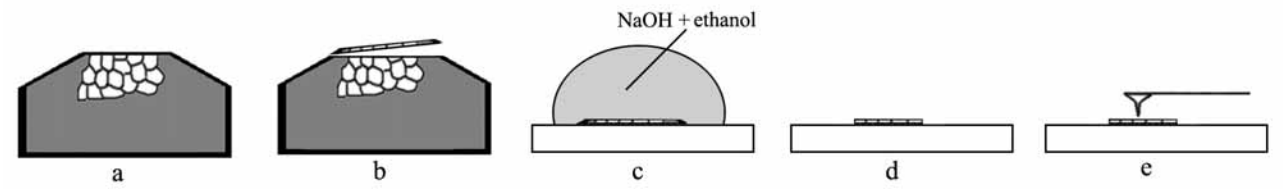

Fig. 2. Diagram showing sample processing and observation. All figures are not to scale.
a. Fossil tissue embedded in Epon resin (gray); b. Thin section cut off the embedded tissue; c. Removal of Epon resin using NaOH in ethanol; d. Fossil tissue free of Epon resin; e. AFM observation on the fossil tissue.

ultrastructures within cells. In the extant material, cytoplasm consists of various membrane systems and organelles, including endoplasmic reticulum (ER) and others (Fineran, 1978; Hall, 1978). Due to the various adhesion strengths between different cytoplasmic components or subcomponents, the fossil cytoplasm tends to break along the weakest binding surfaces when cut with a knife, as in living plants (Moor and Mühlethaler, 1963). Therefore, the heterogeneity of the fossil cytoplasm is indirectly reflected in its microtopography (Plate I, Figs. f-k). A feature that comes to our attention is that some fossil materials appear to be composed of tiny granules (Plate I, Fig. h). The granular microtopography of cytoplasm more or less reflects the original heterogeneity in fossil cells, just as those in the living cells (Moor and Mühlethaler, 1963, figs. 17-29; Fernando et al., 2006, figs. 4j-m, 5a). However, whether the granules seen in this material are composed of macromolecules, as in extant cells under a TEM (Moor and Mühlethaler, 1963, fig. 31), is still an open question.

AFM allows the instrument to map not only the microtopography but also other physical / chemical features of the sample. Besides microtopographical mapping, the AFM also yields phase and amplitude images (Clancy et al., 2000). Phase image includes information related to the chemophysical properties, including composition, adhesion, friction, viscoelasticity, and/or hardness, of the target. Through this process, phase images can highlight the edges and enhance contrast in real-time, and therefore provide information unavailable in other images. In present case phase imaging differentiates the different components of the cytoplasm more clearly than the topography alone (right panels in Plate I, Figs. i-k). The congruence between phase and topography images supports the faithfulness of the imaging. Although we are not so sure exactly which physical or chemical properties contribute to the variations seen in the phase images yet (right panels in Plate I, Figs. i-k), it is apparent that the fossil cytoplasm is composed of components with different physical or chemical properties. It is well known that many plastids have two membranes around, the two membranes, appearing as two parallel curves (Plate I, Fig. i), may well represent the membranes around an organelle. The membrane patches in the cytoplasm (Plate I, Figs. j-k) are reminiscent of membrane system in living cells, such as ER and other organelles. Amplitude image maps the height gradient on the surface of the sample. The image can be taken as the result of the microtopography of the sample as if lit from one side. This way amplitude image highlights some detailed feature invisible in topography alone.

The sensitivity to elevation variation up to nanometer is an apparent advantage of AFM over SEM, using the latter some of the minute topographical variation of fossil cytoplasm was too weak to be detected (Plate I, Fig. d). By scanning using a very flexible probe across the sample surface, AFM collected the three dimensional information as well as chemical/physical features (left panels in Plate I, Figs. i-k). The AFM topographical data can be viewed using software from variable angles (Plate I, Fig. e). AFM amplitude image can be comparable to the SEM image in terms of that both show the view of the topography lit from one side. However, the angle of lighting can be chosen arbitrarily in AFM amplitude image but fixed in SEM image. The disadvantage of AFM compared with SEM is its difficulty in processing drastic changes in height, as in left panel of Plate I, Fig. f. Drastic change in height usually causes unrealistic image in the region nearby.

The pseudomorphological features resulted from sectioning and other processes should be of larger scale and with certain patterns, compared with the tiny observed area and minute variations observed in AFM. The nanoscale features observed here are unlikely to be the result of sectioning or other processing. Therefore errors and artifacts of grinding, sectioning and other processing can be eliminated in the present case.

5 Conclusion

Although the information obtained from fossil cytoplasm is far from satisfactory when compared with the extant cells, this first AFM observation on fossil cytoplasm demonstrates its potential for paleontological research and the heterogeneity within the fossil cytoplasm. The introduction of AFM technology to paleontology and other sciences will definitely promote the research in related areas.

Acknowledgements

We thank Dr. Zhiyan Zhou for his support during this research, Dr. Kaihe Du, Dr. Chuanming Zhou, Ms. Chunzhao Wang, Mr. Yongqiang Mao, Mr. Erjun Zhuo, and Ms. Cuiling He for their help during this program. This study is supported by National Centre for NanoScience and Technology (China), Jiangsu Planned Project for Postdoctoral Research Funds, K.C. Wong Post-doctoral Fellowships, China Postdoctoral Science Foundation (No. 2005037746), State Key Laboratory of Palaeobiology and Stratigraphy (Nanjing Institute of Geology and Palaeontology, CAS), NSFC Program (Nos. 40772006, 40372008, 40632010 and J0630967). This paper is a contribution to IGCP 506.

Manuscript received Nov. 16, 2007
accepted April 7, 2008
edited by Fei Hongcai

References

Canny, M.J., and Huang, C.X., 2006. Leaf water content and palisade cell size. *New Phytologist*, 170: 75–85.

Chen, Y., Cai, J., Zhao, T., Wang, C., Dong, S., Luo, S., and Chen, Z.W., 2005. Atomic force microscopy imaging and 3-D reconstructions of serial thin sections of a single cell and its interior structures. *Ultramicroscopy* 103: 173–182.

Clancy, C.M.R., Krogmeier, J.R., Pawlak, A., Rozanowksa, M., Sarna, T., Dunn, R.C., and Simon, J.D., 2000. Atomic force microscopy and near-field scanning optical microscopy measurements of single human retinal lipofuscin granules. *Journal Physical Chemistry B*, 104: 12098–12101.

Collinson, M.E., Rember, W., Finch, P., Brain, A.P.R., Gupta, N.S., and Pancost, R.D., 2005. Morphological, anatomical, ultrastructural and macromolecular preservation of leaves from the Miocene of Clarkia, Idaho, USA, 15th Goldschmidt Conference. Cambridge Publications, Moscow, Idaho.

Darrah, W.C., 1938. A remarkable fossil *Selaginella* with preserved female gametophytes. *Botanical Museum Leaflet Harvard University*, 6: 113–135.

Eisenack, A., 1965. Erhaltung von Zellen und Zellkernen aus dem Mesozoikum und Paleozoikum. *Natur und Museum*, 95: 473–477.

Fernando, D.R., Batianoff, G.N., Baker, A.J., and Woodrow, I.E., 2006. *In vivo* localization of manganese in the hyperaccumulator *Gossia bidwillii* (Benth) N. Snow & Guymer (Myrtaceae) by cryo-SEM/EDAX. *Plant, Cell and Environment*, 29: 1012–1020.

Fineran, B.A., 1978. Freeze-etching. *In* Hall., J. L. [ed.], Electron microscopy and cytochemistry of plant cells, 279–341. Elsevier/North-Holland Biomedical Press, Amsterdam.

Gould, R.E., 1971. *Lyssoxylon grigsbyi,* a cycad trunk from the upper Triassic of Arizona and New Mexico. *American Journal of Botany*, 58: 239–248.

Hall, J.L., 1978. Electron microscopy and cytochemistry of plant cells. Elsevier/North-Holland Biomedical Press, Amsterdam.

Han, W., Lindsay, S.M., Dlakic, M., and Harrington, R.E., 1997. Kinked DNA. *Nature* 386: 563.

Hizume, K., Yoshimura, S.H., Maruyama, H., Kim, J., Wada, H., and Takeyasu, K., 2002. Chromatin reconstitution: development of a salt-dialysis method monitored by nano-technology. *Arch Histol Cytol.*, 65: 405–413.

Jalili, N., and Laxminarayana, K., 2004. A review of atomic force microscopy imaging systems: application to molecular metrology and biological sciences. *Mechatronics*, 14: 907–945.

Kempe, A., Schop, J.W., Altermann, W., Kudryavtsev, A.B., and Heckl, W.M., 2002. Atomic force microscopy of Precambrian microscopic fossils. *PNAS*, 99: 9117–9120.

Koller, B., Schmitt, J.M. and Tischendorf, G., 2005. Cellular fine structures and histochemical reactions in the tissue of a cypress twig preserved in Baltic amber. *Proceeding of Royal Society B*, 272: 121–126.

Mamay, S.H., 1957. *Biscalitheca*, a new genus of Pennsylvanian coenopterids, based on its fructication. *American Journal of Botany*, 44: 229–239.

Millay, M.A., and Eggert, D.A., 1974. Microgametophyte devo–lopment in the Paleozoic seed fern family Callistophytaceae. *American Journal of Botany*, 61: 1067–1075.

Moor, H., and Mühlethaler, K., 1963. Fine structure in frozen-etched yeast cells. *Journal of Cell Biology*, 17: 609–628.

Muys, J.J., Alkaisi, M.M., Evans, J.J., Melville, D.O.S., Nagase, J., Parguez, G.M., and Sykes, P., 2006. Cellular transfer and AFM imaging of cancer cells using Bioimprint. *Journal of Nanobiotechnology*, 4: 1.

Niklas, K.J., Brown, R.M., Santos, R., and Vian, B., 1978. Ultrastructure and cytochemistry of Miocene angiosperm leaf tissues. *Proceedings of the National Academy of Sciences, United States*, 75: 3263–3267.

Ozerov, I.A., Zhinkina, N.A., Efimov, A.M., Machs, E.M., and Rodionov, A.V., 2006. Feulgen-positive staining of the cell nuclei in fossilized leaf and fruit tissues of the lower Eocene Myrtaceae. *Botanical Journal Linnean Society*, 150: 315–321.

Satterthwait, D.F., and Schopf, J.W., 1972. Structurally preserved phloem zone tissue in *Rhynia*. *American Journal of Botany*, 59: 373–376.

Schönhut, K., Vann, D.R., and LePage, B.A., 2004. Cytological and ultrastructural preservations in Eocene *Metasequoia* leaves from the Canadian High Arctic. *American Journal of Botany*, 91: 816–824.

Taylor, T.N., and Millay, M.A., 1977. Structurally preserved fossil cell contents. *Transaction of American Microscope Society*, 96: 390–393.

Tiribilli, B., Bani, D., Quercioli, F., Ghirelli, A., and Vassalli, M., 2005. Atomic force microscopy of histological sections using a chemical etching method. *Ultramicroscopy*, 102: 227–232.

Wang, X., 2004. Plant cytoplasm preserved by lightning. *Tissue and Cell*, 36: 351–360.

Wang, X., 2006. A chemical signal possibly related to physiology in fossil cells detected by energy dispersive X-ray microanalysis. *Tissue and Cell*, 38: 43–51.

Wang, X., 2007. High temperature as a mechanism for plant cytoplasm preservation in fossils. *Acta Geologica Sinica* (English version), 81: 183–193.

Wang, X., and Cui, J., 2007. The first observation on plant cell fossils in China. *Acta Geologica Sinica* (English version), 81: 16–22.

Wang, X., Liu, W., Cui, J., and Du, K., 2007. Palaeontological evidence for membrane fusion between a unit membrane and a half-unit membrane. *Molecular Membrane Biology*, 24: 496–506.

Yoshimura, S.H., Kim, J., and Takeyasu, K., 2003. On-substrate lysis treatment combined with scanning probe microscopy revealed chromosome structures in eukaryotes and prokaryotes. *Journal of Electron Microscopy*, 52: 415–423.

Plate I AFM and other observations of the cytoplasm in a cone scale

a. A general view of the cone isolated from the embedding sediment. Bar = 2 mm.
b. A thin section of the cone scale using the light microscope. Note the dark-colored cells and light-colored cell walls around the cells in this unstained section. Bar = 50 μm.
c. A view of the same material shown in Fig. b using the SEM. Note most of the cell contents are preserved in the lumina. Section thickness about 2 μm. Bar = 50 μm.
d. A detailed view of the (white) rectangular region in Fig. c using the SEM. Bar = 5 μm.
e. Cross sections of the cell in Fig. h along the line 1 and 2. They show the microtopographical variation along the lines.
f. A view of the square region shown in Fig. d using the AFM. Area = 20 μm × 20 μm.
g. A detailed view of the rectangular region in Fig. f using the AFM. Note the central region (rectangle) with different features. Area = 7 μm × 7 μm.
h. A detailed view of the rectangular region in Fig. g using the AFM. Note the granules in the central region. Two section analyses are done along the line and the result is shown in Fig. e. Area = 4 μm × 4 μm.
i. AFM topographical (left panel) and phase (right panel) images of a part of cytoplasm. Note the two membranes two parallel curves around an organelle in the topographical image (arrows) and their counterparts in the phase image. Area = 2.05 μm × 2.05 μm.
j. AFM topographical (left panel) and phase (right panel) images of a portion of a cell. Note the patchy configuration of subcellular structures. Area = .24 μm × 9.24 μm.
k. A detailed AFM topographical (left panel) and phase (right panel) images of the rectangular portion of the cell in Fig. j. Note the raised patchy. membrane and the lower region around it. Area = 3 μm × 3 μm.